frontiers | Frontiers in Earth Science

TYPE Original Research
PUBLISHED 04 July 2025
DOI 10.3389/feart.2025.1585388

Check for updates

OPEN ACCESS

EDITED BY
Davide Tiranti,
Agenzia Regionale per la Protezione Ambientale del Piemonte (Arpa Piemonte), Italy

REVIEWED BY
Wei-Chia Hung,
National Yang Ming Chiao Tung University, Taiwan
Dora Celia Carreon-Freyre,
Universidad Nacional Autonoma de Mexico, Mexico

*CORRESPONDENCE
Daniela Ruberti,
daniela.ruberti@unicampania.it

RECEIVED 28 February 2025
ACCEPTED 03 June 2025
PUBLISHED 04 July 2025

CITATION
Buffardi C, Minderhoud PSJ, Mandolini A and Ruberti D (2025) Characterizing Holocene sediments for assessing coastal-deltaic subsidence: the role of cone penetration tests and geomechanics.
Front. Earth Sci. 13:1585388.
doi: 10.3389/feart.2025.1585388

Characterizing Holocene sediments for assessing coastal-deltaic subsidence: the role of cone penetration tests and geomechanics

Carla Buffardi[1], Philip S. J. Minderhoud[2,3,4], Alessandro Mandolini[1] and Daniela Ruberti[1]*

[1]Department of Engineering, University of Campania L. Vanvitelli, Caserta, Italy, [2]Soil Geography and Landscape Group, Wageningen University & Research, Wageningen, Netherlands, [3]Department of Civil, Environmental and Architectural Engineering, University of Padova, Padova, Italy, [4]Department of Subsurface and Groundwater Systems, Deltares Research Institute, Utrecht, Netherlands

River deltas and coastal-deltaic plains are, by nature, subjected to land subsidence from the consolidation of shallow, unconsolidated Holocene sediments. The spatio-temporal potential and occurrence of shallow coastal-deltaic subsidence—caused by both natural and anthropogenic factors—are highly dependent on geological and geotechnical Holocene stratigraphic characteristics. In this study, we utilized new CPT/CPTu measurements from the Volturno coastal deltaic plain (northern Campania, Italy) to geomechanically characterize the Holocene sedimentary facies, highlighting the great potential of this approach. The results reveal that although different facies associations may share similar lithologic compositions, their geotechnical behaviors may be strikingly dissimilar. These differences are attributable to varying paleo-depositional environments and sedimentary processes that create distinctive geomechanical fingerprints governing their consolidation behavior. These variable characteristics underlie, and in part explain, the spatial patterns in observed subsidence rates. The increased geomechanical insights advance our understanding of the spatio-temporal consolidation of the Holocene sedimentary sequence and its various depositional facies beyond standard lithological geotechnical characterization. In addition, they also enable further explorations, such as simulating 3D Holocene delta growth and evolutionary sediment compaction using numerical models.

KEYWORDS

Volturno River, alluvial and delta-coastal plain, southern Italy, land subsidence, CPT–CPTu, sediment compaction, facies characterization

1 Introduction

Land subsidence (LS) is the slow or sudden sinking of a ground surface, a complex phenomenon due to the consolidation of sediments and, thus, the subsurface movement of earth materials as a result of increasing effective stress (Hu et al., 2004).

The areas affected by this phenomenon are particularly monitored and studied as it can trigger economic, social, environmental, geological, and hydrogeological threats (Stouthamer et al., 2020). Although LS affects different geographic settings, it represents a crucial problem in alluvial–coastal and delta settings where this phenomenon seriously affects marine–coastal environments, contributing to the loss of coastal lowlands, increasing the vulnerability to flooding by tides and storm surges, and leading to the destruction of infrastructures (Ericson et al., 2006). From a hydrogeological point of view, LS may lead to variations in porosity and permeability, an increase in the thickness of the unsaturated zone, and the salinization of the aquifer (Carbognin et al., 2010; Higgins, 2016; Minderhoud et al., 2018).

LS is influenced by a wide range of causes, both natural and anthropogenic, and this diversity in origin leads to significant variability in subsidence rates across different geographical regions of the world (Bagheri-Gavkosh et al., 2021). The main natural causes include tectonic movements, glacial isostatic adjustments, earthquakes, and the geological and geotechnical characteristics of the different layers that lead to their chemical and physical transformation, such as sediment compaction or the oxidation of the peat (Galloway et al., 2000; Van Asselen et al., 2011; Yang et al., 2014; Higgins, 2016). Gas exploitation, mining, the loads of increasing urbanization, and overexploitation of groundwater are the most diffuse anthropogenic causes (Galloway and Burbey, 2011; Jones et al., 2016; Calabrese et al., 2021). Among them, the latter alone is responsible for 41% of subsidence cases (Bagheri-Gavkosh et al., 2021). Generally, natural causes lead to slower subsidence, resulting in the sinking of a few centimeters in a year, except in the case of some exceptional events such as earthquakes; anthropogenic subsidence, on the other hand, is much more significant, with rates that may reach several meters over the decades (Shirzaei et al., 2021). Sometimes, anthropogenic activities can accelerate some natural processes such as sediment and aquifer compaction; these processes can also depend on human activities and rapid urbanization, including groundwater extraction (Wu et al., 2022). In the last century alone, subsidence caused by groundwater depletion has affected 200 different locations in 34 different countries, and it is estimated to affect an area of 2.2 million km^2 in 2040 and 19% of the global population (Herrera-García et al., 2021).

Understanding LS requires a multidisciplinary approach as the phenomenon does not occur uniformly everywhere. The diversity in subsidence processes has inspired numerous studies and reviews to increase our understanding of the issue (Shirzaei et al., 2021; Herrera-García et al., 2021; Buffardi and Ruberti, 2023; Huning et al., 2024; Pedretti et al., 2024; Thomas et al., 2024). One of the main outcomes of these reviews is that subsidence is not a simple phenomenon but rather covers multiple scientific disciplines, including geomechanics, hydrogeology, and geology.

As land subsidence is governed by processes in the subsurface, its site-specific geological and geotechnical characteristics dictate potential rates, especially in unconsolidated, subsidence-prone settings such as coastal plains and river deltas. These geologically young areas were formed during the Holocene, and the soft, compressible nature of their shallow subsurface sediments makes them exceptionally susceptible to LS (Dassargues et al., 1991; Liu and Huang, 2013; Bozzano et al., 2015; Törnqvist et al., 2008; Van Asselen et al., 2009; Da Lio and Tosi, 2018; Tosi et al., 2018; Tzampoglou and Loupasakis, 2018; Zoccarato et al., 2018; Amato et al., 2020; Buffardi et al., 2021). Fine-grained lithologies, such as clay and peat, are abundant in the Holocene stratigraphy and are prone to compact under loading (Törnqvist et al., 2008; Van Asselen et al., 2011; Koster et al., 2016; Zoccarato et al., 2018) and oxidation of organic matter (van Asselen et al., 2009), leading to severe volumetric loss and, consequently, LS. Knowledge of the physical characteristics of these materials is important to assess the subsidence potential, forecast future trends, and manage the impacts (Koster et al., 2018).

An effective method to determine the geological and geotechnical stratigraphic characteristics is the cone penetration test (CPT), which was developed in the 1930s in the Netherlands. The test was initially used to measure sediment penetration resistance during pile foundation investigations (Buisman, 1940). Afterward, following technical improvements, it was also used for lithological classification (Begemann, 1965) and to identify the soil type and soil stratigraphy through the two main measurable parameters, namely, the penetration resistance at the penetrometer tip (q_c) and the friction along the tool sleeve (f_s) (Amorosi and Marchi, 1999). In the 1970s, further advancements were introduced such as the measurement of pore-water pressure (u). These parameters are essential for geotechnical analyses as they characterize soil behavior, stability, and bearing capacity. For example, based on the values of f_s, it is possible to derive information about the presence of fine-grained soils, such as silts and clays, which have a pronounced effect on soil properties (Cai et al., 2019).

Compared with other types of investigations, both *in situ* and in the laboratory, the CPTs are fast, replicable, and less expensive. In addition, CPTs offer continuous data collection as the cone penetrates the soil, offering a detailed picture of the stratigraphy and soil type variations (Mohammad et al., 1999; Robertson, 2010; 2016). The results of the CPT/CPTu are used for different applications, such as for evaluating liquefaction due to earthquakes (Idriss and Boulanger, 2006; Boumpoulis et al., 2021; Geyin et al., 2021; Guan et al., 2021; Guo et al., 2022; Zhao et al., 2022), obtaining the thermal properties of saturated soils (Vardon and Peuchen, 2021), estimating the bearing capacity of foundations (El-Reedy, 2015; Eslami et al., 2020; Heidarie Golafzani et al., 2020), or characterizing aquifer architecture. CPT data have also been successfully used to evaluate past and present compaction of peat layers due to overburden loading or water-table lowering (Koster et al., 2016; Koster et al., 2018).

The data from CPT(u)s provide an excellent resource to support subsurface reconstruction, especially in the coastal-deltaic and alluvial plains, as demonstrated by many studies that have applied CPT(u) data to characterize unconsolidated sediments (Anagnostopoulos et al., 2003; Lafuerza et al., 2005; Choi and Kim, 2006; Bombasaro and Kasper, 2016; Koster et al., 2018; Yang et al., 2021). These studies aim to develop and provide methods specifically for coastal-deltaic and alluvial plains. Most of them focus on the lithological characterization of a specific geographical area (Amorosi and Marchi, 1999; Lafuerza et al., 2005; and Styllas, 2014), while only few also consider the different depositional facies that can be found in these complex ecosystems (Zhang et al., 2018). Campo et al. (2023) aimed to provide a widely exportable approach for studying coastal-deltaic and alluvial plains. They demonstrated the possibility of associating soil types deduced from CPT data to Holocene facies association, thus offering an easy-to-use and economical tool to characterize the lithostratigraphic structure of the subsoil in the different European coastal-deltaic and alluvial plains.

Land subsidence research often specifically focuses on Holocene sediments in coastal-alluvial settings as these represent the youngest and most superficial deposits that are prone to the highest rates of consolidation. They contain the recent geological history of depositional settings originating from the various phases of retrogradation, aggradation, and progradation that characterized the Holocene formation of extensive coastal floodplains worldwide (Syvitski et al., 2022; Anthony et al., 2024). In these depositional environments, a range of different natural processes takes place (Miall, 2018), and sedimentation and compaction are intrinsically connected with their growth and internal dynamics (Zoccarato et al., 2018). The study of these environments is essential because they are dynamic systems, constantly evolving due to natural sedimentation and compaction processes, which are influenced by shifts in climate, sediment supply, and extreme events such as storms and tsunamis (Switzer et al., 2012; Ranasinghe, 2020). They are also rich in fertile soils and (ground)water availability, and they have been sites of colonization, agricultural practices, and natural resource exploitation for a long time and, consequently, experienced large-scale land-use and geomorphological changes (Brückner et al., 2005; Devillers et al., 2019; Anthony et al., 2024). These anthropogenic actions can accelerate some of the undesired natural processes, such as coastal erosion and subsidence in sensitive areas such as deltas (Coelho et al., 2009; Lazarus et al., 2016; Mentaschi et al., 2018); for example, subsidence processes can be triggered and enhanced by land-use change as a result of the concomitance of increased agricultural production, population growth, and urbanization in deltaic areas (Minderhoud et al., 2018). The complex origin of depositional environments, coupled with the interplay of natural and anthropogenic factors and their combination, has placed them as focal points in numerous studies worldwide (Stiros, 2001; Törnqvist et al., 2008; Syvitski et al., 2009; Ruberti et al., 2017; Shirzaei et al., 2021; Schmitt and Minderhoud, 2023; Scown et al., 2023; Becker et al., 2024).

The Volturno delta plain in the south of Italy, along the eastern Tyrrhenian Sea, shares a Holocene geological evolution similar to that of other alluvial coastal plains worldwide (Figure 1); it was mainly formed since the middle-Holocene, following the progressive lowering of the post-glacial sea-level rise, which created conditions favorable for early aggradation (6.5–4.5 ky BP) and late-stage progradation (<4.5 ky). This allowed the formation of a wave-dominated delta system, with flanking strandplains forming beach-dune ridges that partially enclosed lagoonal–marshy areas (Ruberti et al., 2022, references therein).

This environmental setting is undergoing many undesired changes, such as landscape fragmentation and reduction of biodiversity and environmental quality. It also experiences high rates of land subsidence (Figure 1b), ranging between −5 and −25 mm/yr in an area of approximately 750 kmq across the Volturno River (Matano et al., 2018; Buffardi et al., 2021) and mainly related to the distribution of the Holocene sediments, as documented in several alluvial and deltaic-coastal plains worldwide (Meckel et al., 2006; Phien-wej et al., 2006; Campolunghi et al., 2007; Törnqvist et al., 2008; Van Asselen, 2011; Teatini et al., 2011; 2012; Sarti et al., 2012; Higgins et al., 2014; Jones et al., 2016; Koster et al., 2018; Bruno et al., 2020).

Different studies have been conducted on the area to understand the relationship between land-use changes and landscape pattern (Ruberti and Vigliotti, 2017) or to quantify the coastal inundation risk (Aucelli et al., 2017). Detailed geological studies used dating, boreholes, and seismic data to characterize the Holocene sediments and the underlying depositional units (Amorosi et al., 2012; Corrado et al., 2020; Ruberti et al., 2020; Ruberti et al., 2022). The lithology and related depositional environments of the Volturno delta were reconstructed in recent studies (Buffardi et al., 2021; Ruberti et al., 2022). However, to date, it remains unclear how the paleo-depositional evolution of the Volturno delta has influenced the geomechanical behavioral characteristics of these sediments, thereby governing past and present-day sediment (auto)compaction.

This study aims to assess the variability in the geomechanical characteristics of different lithologies belonging to various depositional facies in the coastal–alluvial plain of the Volturno River by employing new, recently acquired CPT(u) and borehole data. The CPT(u) data were cataloged and analyzed based on the lithologies, depositional facies, and penetrometric facies that make up the stratigraphic architecture of the plain. This yielded the penetrometric parameter ranges of each lithofacies in the coastal-deltaic and alluvial plains, offering valuable insights into the geomechanical characteristics of the subsurface and its susceptibility to compaction. It also provides a foundation for further research aimed at quantifying the current and potential future dynamics of (auto)compaction and land subsidence in the region. In addition, the method may be valuable for investigating and characterizing similar coastal-deltaic plains elsewhere in the world.

2 Study area

Located in Southern Italy, the Volturno coastal plain corresponds to the northern Campanian Plain, a graben or half-graben structure in which thousands of meters of Quaternary sediments have accumulated (Figure 1a). Numerous studies have characterized the stratigraphic evolution of this plain through borehole data, radiocarbon dating, and paleoenvironmental indicators (Romano et al., 1994; Santangelo et al., 2010; Amorosi et al., 2012; 2013; Ruberti et al., 2014; Sacchi et al., 2014; Santangelo et al., 2017; Matano et al., 2018; Ruberti et al., 2018a; Corrado et al., 2020; Ruberti et al., 2020).

The evolution of the plain was strongly controlled by intense volcanic activity occurring on the northern and western borders of the plain and by the river and coastal sedimentary activity. One of the most important pyroclastic eruptions occurred in the Campi Flegrei, on the Tyrrhenian side of the plain, which covered the whole area with thick volcanic tuff depositions (the Campania Gray Tuff, CGT; ~39 Ky; Vivo et al., 2001). Following the sea-level decrease associated with the eustatic regression during the Last Glacial Maximum (LGM), the shoreline shifted seaward, and paralic-shallow marine depositional systems underwent a forced regression. Simultaneously, the paleo-rivers flowing across the plain initiated two major downcuttings in the CGT unit, which correspond to the present Volturno River and the Regi Lagni canal (the former Clanio River), leading to the formation of an incised valley that is 15–20 km wide and up to 30 m deep in the depocenter (Amorosi et al., 2012; Sacchi et al., 2014; Ruberti et al., 2018b; 2022; Buffardi et al., 2021).

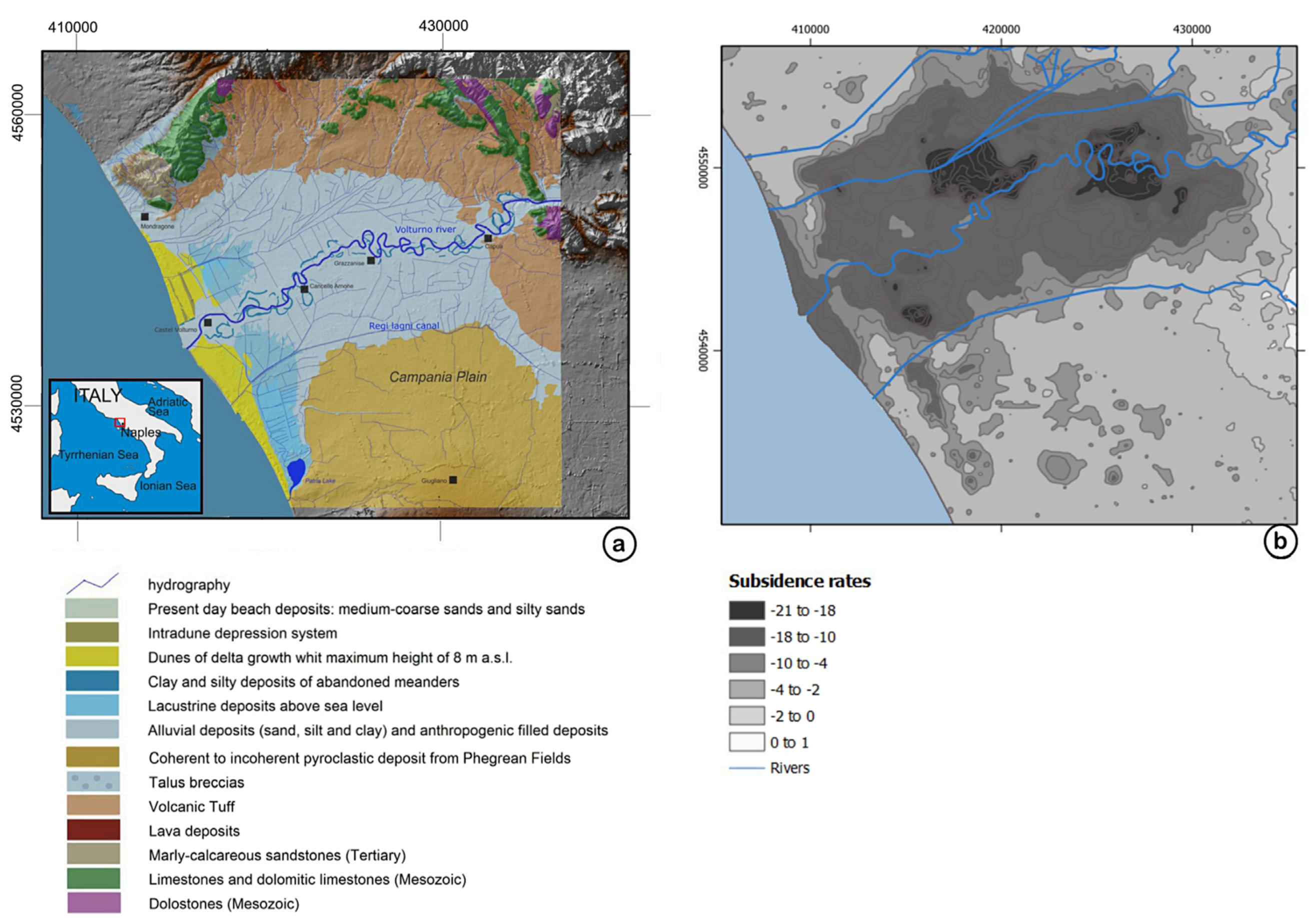

FIGURE 1
Location map of the study area (red box in the map of Italy). **(a)** Schematic geologic map of the study area (based on Buffardi et al., 2021, modified) plotted on the DTM; **(b)** cumulative vertical ground displacement (based on Ruberti et al., 2022).

Above the tuff, the sedimentary infill of the Volturno plain is characterized by a Holocene sedimentary sequence, consisting of a succession of transitional and alluvial facies in a transgressive–regressive sequence (Ruberti et al., 2022). The two profiles reported in Figure 2 highlight the latero-vertical arrangement of the facies and the configuration of the tuff top surface in two cross-sections parallel and perpendicular to the coastline.

As previously stated, the main construction of the present-day delta and coastal setting started at approximately 6.5 ky cal BP, when a phase of coastal progradation occurred, leading to the development of a wave-dominated delta system (Figure 3). A seaward shift of depositional systems followed the post-glacial early aggradation and later-stage progradation (Sacchi et al., 2014; Margaritelli et al., 2016; Misuraca et al., 2018). This, in turn, led to a rapid infilling of the accommodation space over the former incised valley, resulting in the formation of the modern Volturno alluvial plain, coastal lagoons, and beach barrier systems. South of the Volturno delta mouth, a large lagoon–swamp system is documented, likely fed by the ancient Clanio River (now Regi Lagni canal) (Ruberti et al., 2022). These beach and lagoon environments persisted in the present coastal zone until Roman times. The outline of the paleo-gulf and the beach-dune system remains visible in the current topography (Ruberti et al., 2022).

An important role in the recent formation of the plain was played by the anthropic actions, which began during the Spanish vice-kingdom (Ruberti et al., 2022). The former Clanio River was canalized to avoid the continuous flooding of a large part of the inner Neapolitan coastal area. In addition, most of the marshy areas were reclaimed starting in the early 1800s, a process that continued for nearly a century, allowing massive urbanization that has affected the entire coastal area in the second half of the 20th century (Ruberti and Vigliotti, 2017). These landscape and land-use changes resulted in severe coastal erosion (Ruberti et al., 2017; Donadio et al., 2018), environmental pollution, and aquifer salinization (Verde et al., 2013; Roviello et al., 2020; Busico et al., 2021; Colombani et al., 2024).

3 Materials and methods

The integration of geological and geotechnical data is a key objective of this study; the following sections describe the steps carried out to perform geological reconstruction and the procedure

10.3389/feart.2025.1585388

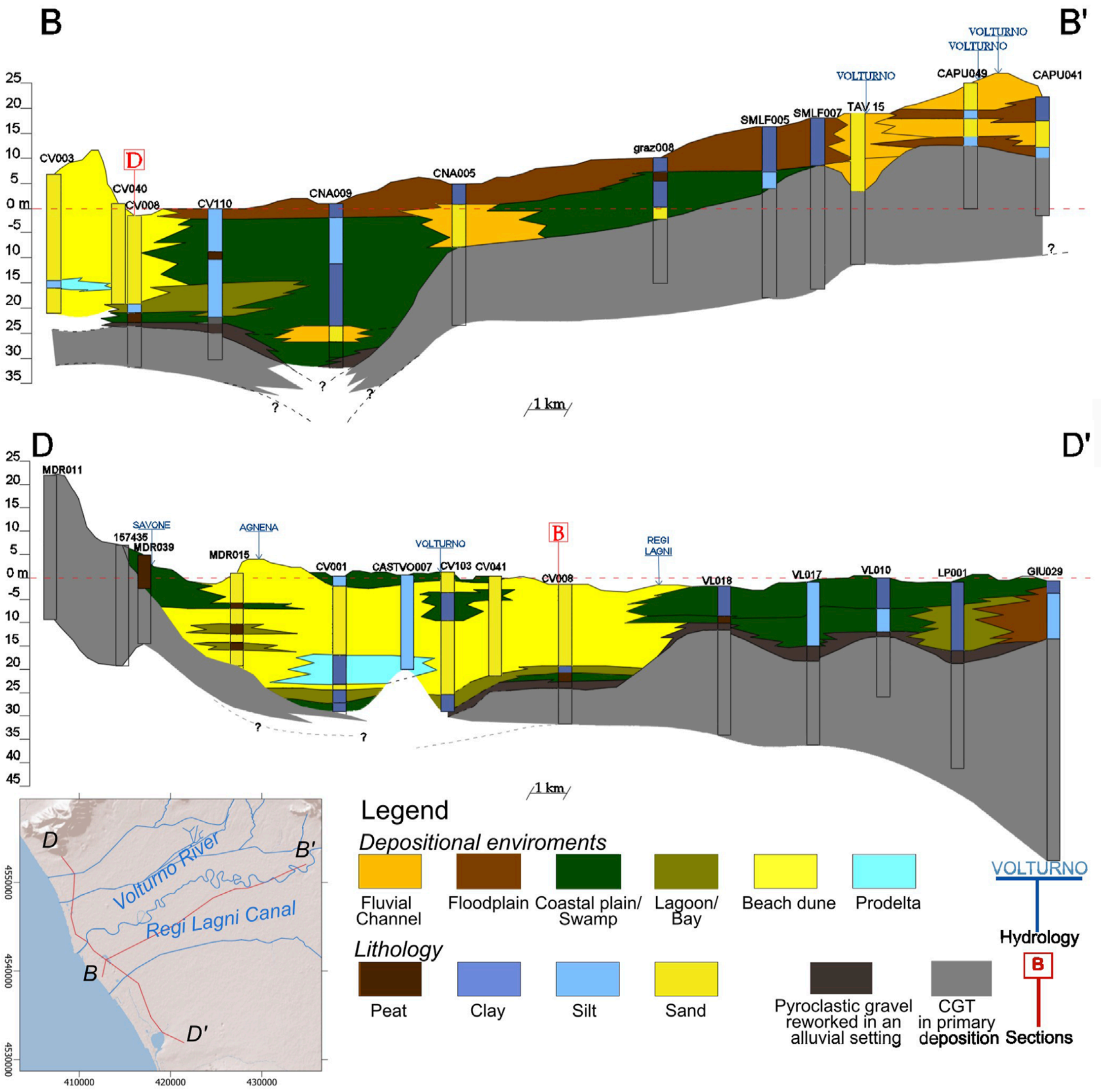

FIGURE 2
Geological profiles showing the reconstruction of the depositional environments; lithological data are reported for each stratigraphic borehole.

used to derive geotechnical parameters, which were essential to assess the geotechnical behavior of the sediments in the study area.

3.1 Geological reconstruction

The first step was to create a detailed geological reconstruction based on the lithological and depositional composition of the subsoil. More than 1,500 borehole data points (mostly up to 20–30 m in depth) located along the lower Volturno plain (Figure 4) were analyzed by Buffardi et al. (2021) and Ruberti et al. (2022) to reconstruct the lithological and depositional architecture and assess their spatial variability.

The borehole data were further utilized to create a quasi-3D interpolation using Surfer software. Based on the average depth of the tuff upper surface and the available geochronological data, four layers at different depths from the ground level (−15, −10, −5, and −2 m, respectively) were identified. On each layer, the depositional environments reconstructed through the stratigraphic analysis of the well-log data were characterized. The results highlight the spatial distribution of the different depositional environments at each defined depth and provide information about the construction phase of the present deltaic and coastal environment.

3.2 Geotechnical analysis

The analysis of the geotechnical parameters involved the interpretation of 32 CPTs and five CPTus (Figure 5), the latter of which were obtained by a specific survey carried out for this study. Tests performed next to boreholes for which an accurate lithostratigraphic reconstruction was available were selected. Interpretation was carried out using “CPeT-IT v.3.7.1.12 CPT

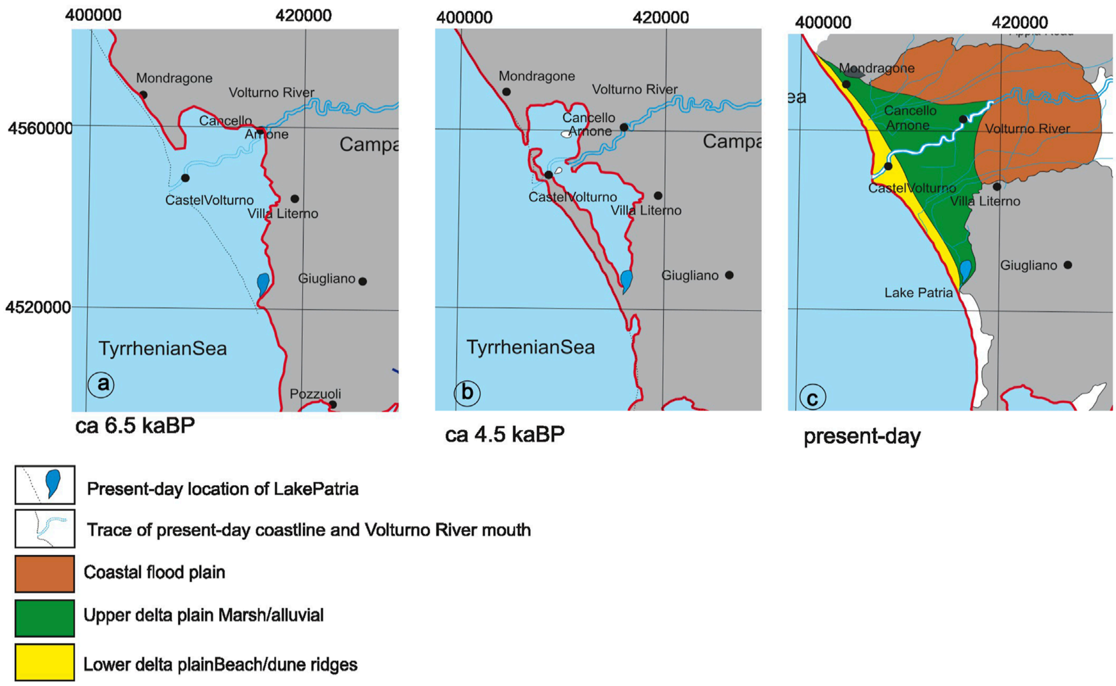

FIGURE 3
Paleo-evolution of the Volturno delta plain: **(a, b)** reconstruction of the approximate coastline evolution since the beginning of the progradational phase started approximately at 6.5 ka BP, according to Ruberti et al. (2022); **(c)** present-day setting of the Volturno delta plain.

interpretation software" with the necessary input data: q_c and f_s and, in the case of CPTus, u as well.

In this study, the normalized CPT soil behavior type (SBTn) by Robertson (1990) was used to characterize the depositional facies. This approach plots normalized cone resistance, Q_t (Equation 1), *versus* FR (Equation 2), the normalized friction ratio:

$$Q_t = \frac{q_c - \sigma_{vo}}{\sigma'_{vo}}, \tag{1}$$

$$FR(\%) = \frac{f_s}{q_c - \sigma_{vo}} * 100, \tag{2}$$

where σ_{vo} is the *in situ* total vertical stress, σ'_{vo} is the *in situ* effective vertical stress, and Q_t is the corrected cone resistance for pore water effects.

By using Q_t (Equation 1) and FR (Equation 2) values, it is possible to derive the soil behavior index, I_C (Equation 3), which is defined as follows:

$$I_C = \left((3.47 - log\,Q_t)^2 + (logFR + 1.22)^2\right)^{0.5}. \tag{3}$$

The derived I_C values allow for the classification of soils, as depicted in Table 1.

Due to the availability of 36 boreholes close to CPTs (Figure 5), it was then possible to not only check whether the I_C values were in line with subsoil stratigraphy from boreholes but also to assign representative quantitative values that establish correlations between quantitative parameters (q_c and FR) and the related soil layer. In particular, the adopted procedure was divided into three steps.

Step 1: lithological interpretations were developed based on cone resistance, normal friction ratio, and SBTn index data from the CPTs for which good stratigraphic control was available.
Step 2: a facies interpretation was attributed to each lithology based on stratigraphic borehole data close to the penetrometric survey.
Step 3: the geotechnical parameters were correlated with each lithofacies unit.

4 Depositional facies and CPT characterization

The characterization of the Holocene alluvial and coastal deposits of the Volturno plain was based on borehole log data and sedimentological and paleontological analyses (Amorosi et al., 2012; Sacchi et al., 2014; Ruberti et al., 2022). Six main depositional facies are considered in this study.

4.1 Alluvial plain deposits

Coarse-to-fine gray–brown sands are locally recognized on top of the CGT unit. Sub-spherical, millimeter-sized white pumice and scoriaceous lapilli are the main components of these sands. Radiometric dating carried out by Amorosi et al. (2012) on the intercalated silts highlighted an age of approximately 37 ky BP; their stratigraphic position suggests that these deposits represent fluvial

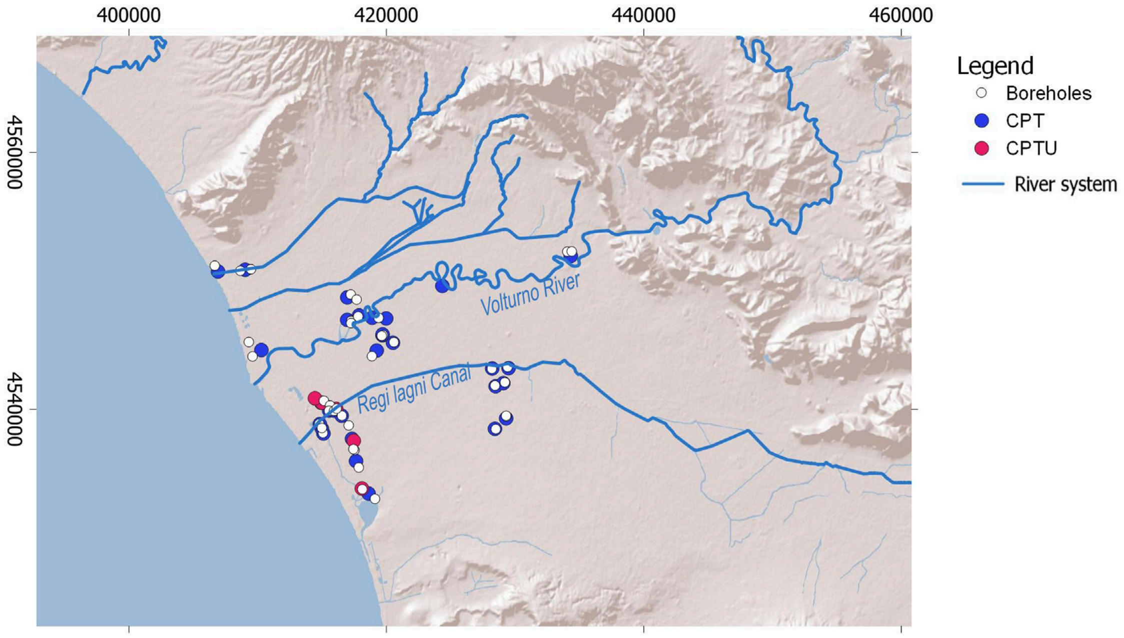

FIGURE 4
Location of the boreholes used in the study.

deposits flooring the paleovalley or fluvial terraces related to the last glacial period.

Modern alluvial plain deposits occur on top of the Holocene succession and characterize a large part of the current Volturno plain. These deposits are characterized mainly by silt and clay, often pedogenized, and contain plant fragments; small rounded pumice; and, sometimes, small pulmonates. They represent a floodplain deposition. In some cases, coarse-to-medium, moderately sorted sand bodies can be distinguished, which can be attributed to fluvial channels, while the successions of very fine sand and silt that are associated with these bodies could represent crevasse/levee deposits.

4.2 Delta plain deposits

This depositional system includes facies associations that formed in freshwater or brackish water environments and constitutes a large part of the Holocene succession of the Volturno coastal plain, extending to the central part of the study area.

Gray clays and silts with plant remains and locally abundant organic matter are recognizable; in some areas, small carbonate nodules can be recognized. Pulmonate mollusks are sometimes recognizable. These features have been interpreted as representing a coastal plain environment, which was generally poorly drained. The first deposits resting unconformably on top of the CGT consist of soft, dark clay rich in organic material. They are also observed at different stratigraphic levels. Plant fragments are common, together with freshwater gastropods. Peat layers, up to 2-m thick, occur at different levels. This facies association can be interpreted as a swamp deposit. They laterally pass to alternating layers of silt and sand rich in mollusk shells; small fragments of pumice are locally recognized. Amorosi et al. (2012) described a foraminiferal and ostracod association that, together with the sedimentary characteristics, allows us to interpret these deposits as typical of a brackish lagoonal/estuarine environment.

4.3 Beach/dune deposits

This facies association includes yellow, medium-to-fine, well-sorted sands containing mollusk shells and scattered rounded pumice fragments. It is well-developed in the present coastal setting, reaching up to 30 m in thickness, and is recognized inland up to approximately 15 km from the coast.

4.4 Prodelta deposits

This facies association is recognized only in an area close to the coast, near the current mouth of the Volturno. It is characterized by gray silty clays that remain on the transgressive barrier sands and present thin intercalations of fine sands. According to the stratigraphic position and the composition of the meiofauna, Amorosi et al. (2012) attributed these deposits to an offshore prodelta environment. None of the CPTs reached this interval, and therefore, it was not characterized from a penetrometric point of view.

The reprocessing of depositional data resulted in the output of four new maps (Figure 6), which illustrated the distribution of depositional facies at different depths and relative to the middle Volturno plain up to the current coastline. In this sector of the study area, the maximum thickness and the greatest variability of facies of the Holocene succession are reached; furthermore, the available CPTs reach a maximum depth of 12 m. The maps likely

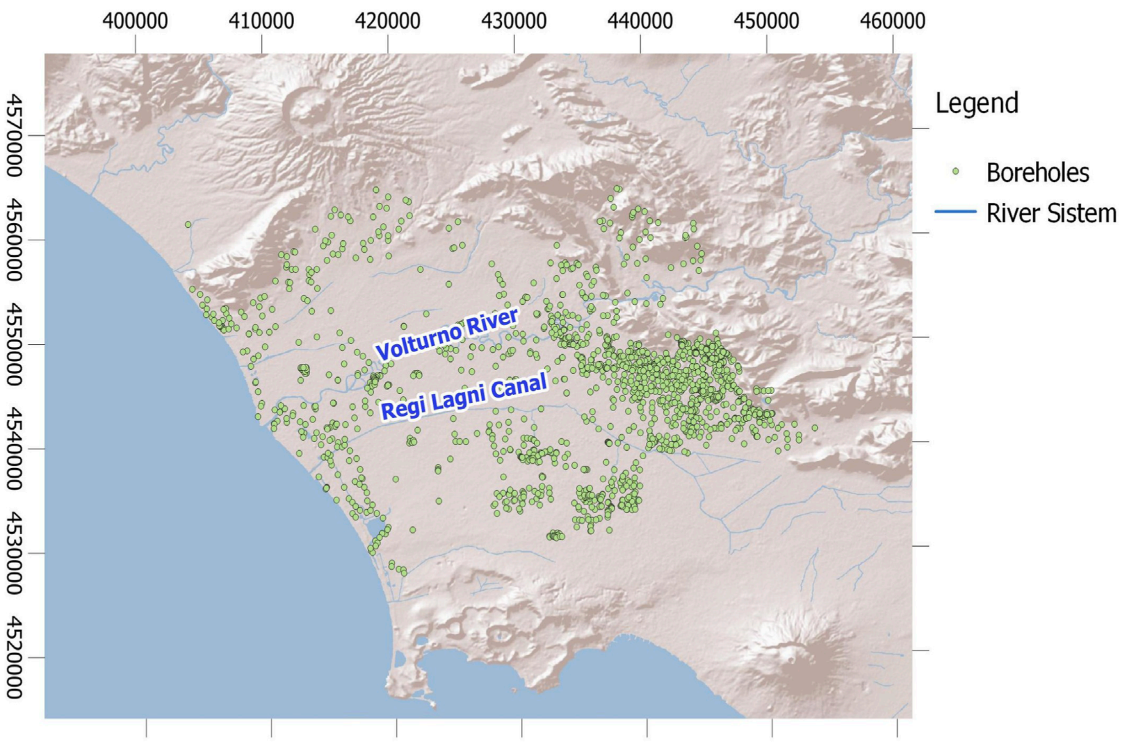

FIGURE 5
Location of the boreholes/cone penetration test used for the analysis.

TABLE 1 Zonation of soil behavior types and the corresponding index (I_C) developed by Robertson (1990) and Robertson (2010).

Zone	Soil behavior type	Ic
1	Sensitive, fine-grained	N/A
2	Organic soils—clay	>3.6
3	Clay—silty clay to clay	2.95–3.6
4	Silt mixtures—clayey silt to silty clay	2.6–2.95
5	Sand mixtures—silty sand to sandy silt	2.05–2.6
6	Sands—clean sand to silty sand	1.31–2.05
7	Gravelly sand to dense sand	<1.31
8	Very stiff sand to clayey sand*	N/A
9	Very stiff fine-grained*	N/A

*Overconsolidated or cemented.

show the spatial extent and organization of the abovementioned environments at different stratigraphic levels. The age attribution can be considered only indicative since the depositional surfaces belong to a transgressive–regressive sequence. However, the maximum age reached by the sediments at the four depths can be considered a reference value and likely corresponds to approximately 8 ka BP. Observing how these zones shift across each map provides insights into the sedimentary evolution and lateral migration of environments.

4.5 CPT characteristics

The comparison of the borehole logs and the geotechnical characteristics reveals noticeable information about the lithological composition of depositional environments. Several stratigraphic logs are characterized by different lithologies and significant changes in geotechnical parameters, even in the presence of the same depositional environment. Lagoonal sediments are composed of sediments with considerable differences in lithology type and grain size (Figure 7a). This is particularly evident in parts where the dominant lithology consists of peat, when the *FR* values increase, or sand, when the q_c values are the highest (Figure 7b). In contrast, in many cases, lithologies remain relatively uniform throughout the log, while the inferred depositional environments change significantly. These changes are usually enhanced by sharp changes in the *FR* and q_c values (Figures 7c,d).

Comparing the data along the plain, the main characteristics for each facies can be summarized as follows.

- The Late Pleistocene alluvial plain is characterized by gray pyroclastic sands that correspond to the upper layers of the tuff reworked in the alluvial setting; they are typified by high q_c values, in a range of 5–15 MPa, whereas the *FR* is generally low, reaching the maximum values of 3%. As

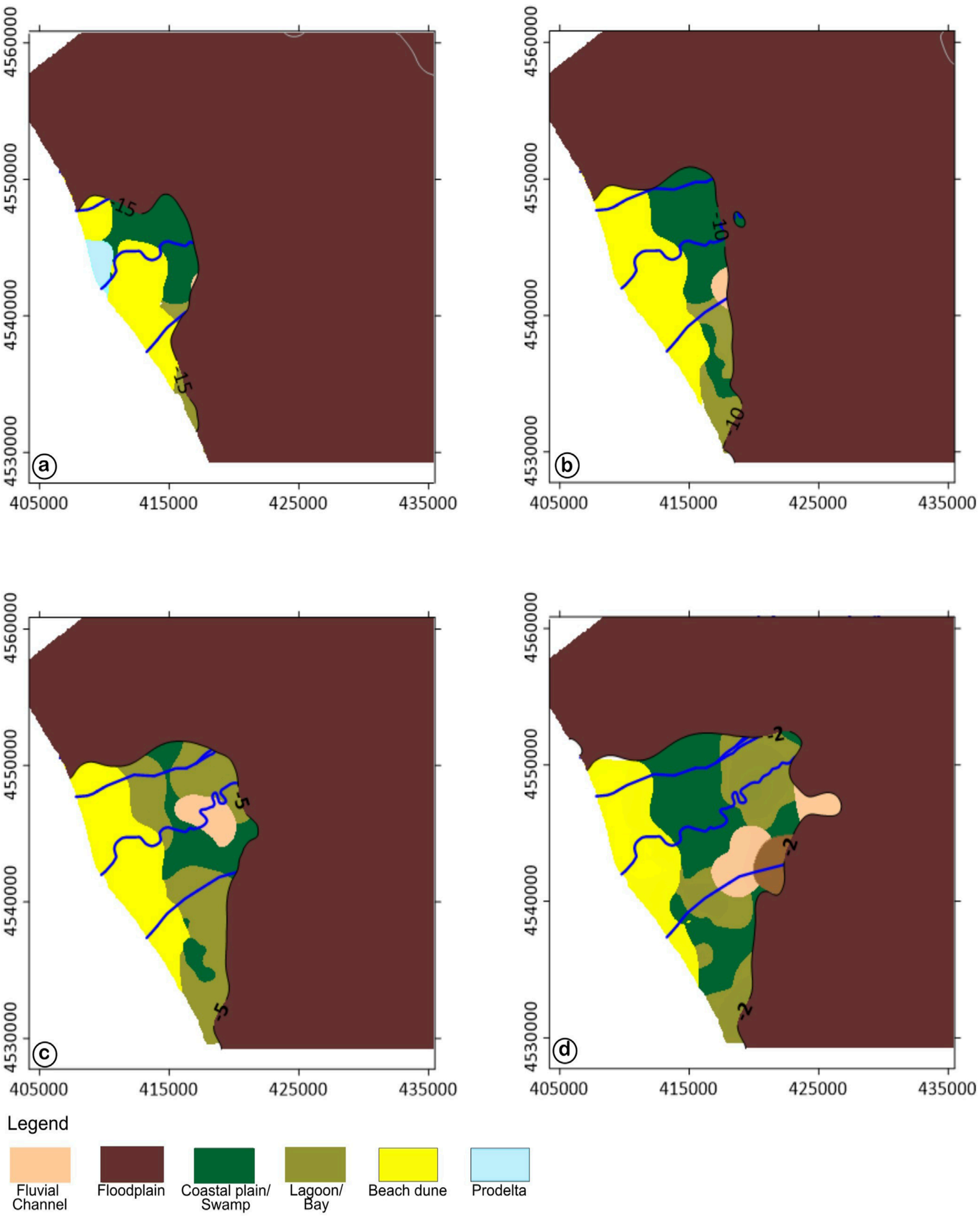

FIGURE 6
Schematic maps showing the distribution of depositional facies at different depths referred to the current sea level, indicated by the following contour lines: **(a)** –15 m.; **(b)** –10 m.; **(c)** –5 m; and **(d)** –2 m. The maps show the spatial extent and organization of the recognized environments at different stratigraphic levels. The maximum age reached by the sediments at the four depths can be considered a reference value and likely corresponds to 8 ka BP.

the underlying tuffaceous substrate is approached, q_c reaches higher values, while the *FR* progressively decreases. Locally thick layers of sandy silt occur, transitioning downward into the tuffaceous substrate, which is characterized by higher *FR* values of approximately 5%.

- The yellow sands, belonging to the beach-dune system, show quite stable q_c values between 5 and 10, with just a few peaks reaching 15 MPa; in addition, *FR* values are almost stable, which is between 1% and 4%. These sands reach high thicknesses, up to 30 m, along the present-day littoral zone.

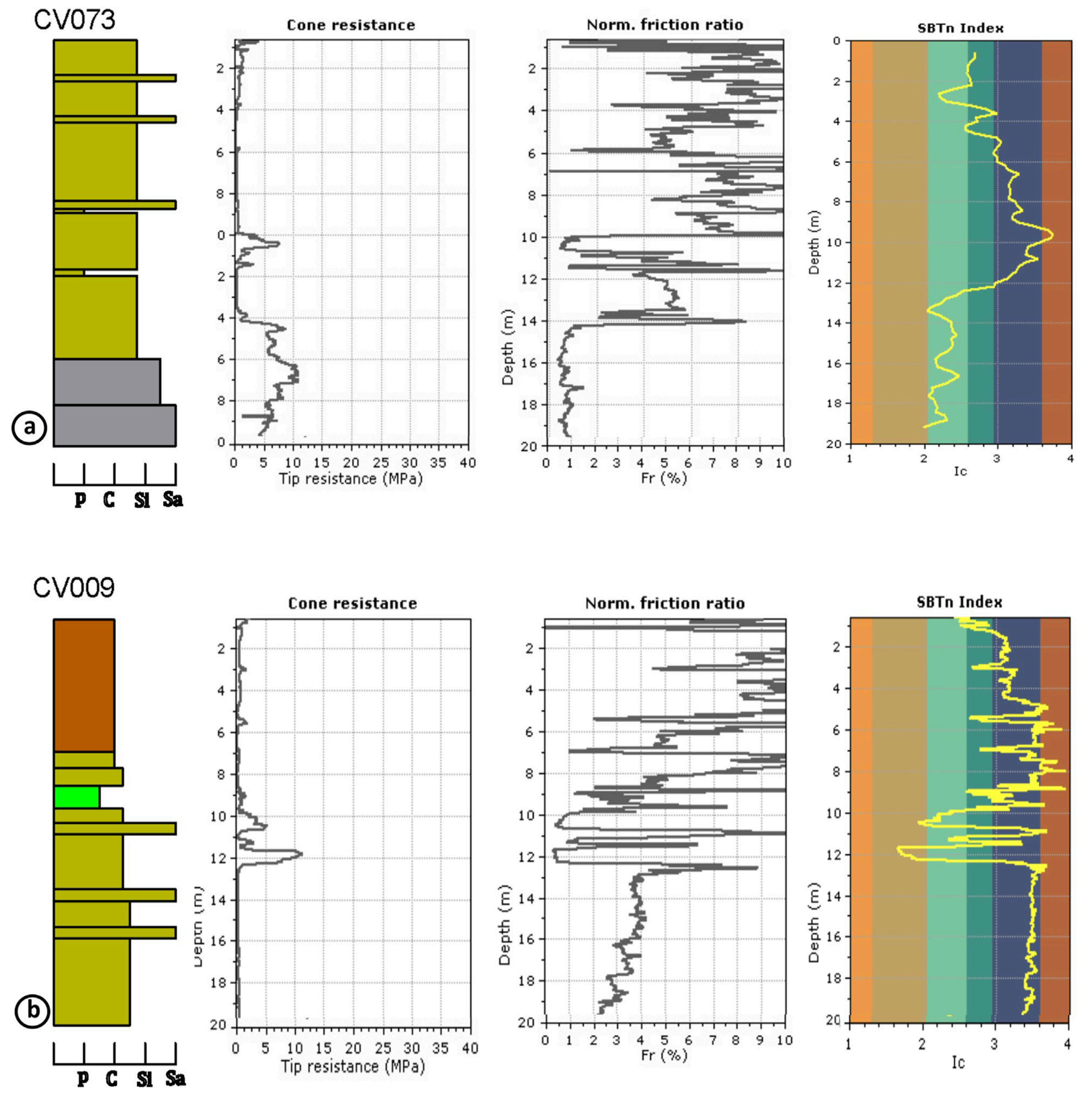

FIGURE 7
(Continued).

- The fluvial channel facies association is composed of gray sand, ranging from fine (locally with silt) to medium sand. The grain size variations result in a wider range of q_c values with respect to the pyroclastic sands, ranging from 0 to 15 MPa, and *FR* values ranging between 2%–4%.
- The floodplain facies association mostly characterizes the innermost part of the plain. It is composed of clay and silty clay, which often contain roots and paleosols. These lithologies are identified by characteristic low values of q_c, an average of 2.5 MPa with minimum values from 0.75 MPa, and a wide range of *Fs* values of 3%–10%.
- The delta plain depositional system comprises the coastal plain, swamp, and lagoon facies association, all of which are generally characterized mainly by clay. In the coastal plain, the clay is mixed with silt characterized by q_c values ranging from 0 to 5 MPa and *FR* ranging from 3% to 7%, and the maximum values can be reached in correspondence with organic matter or roots. The average thickness of the coastal plain deposits is 4 m.
- The clay belonging to the swamp environment is usually dark colored and, at times, alternates with peat layers. This characteristic can be recognized in the recorded *FR* values that reflect the peat content, showing peaks. This facies association is less thick than other deposits.

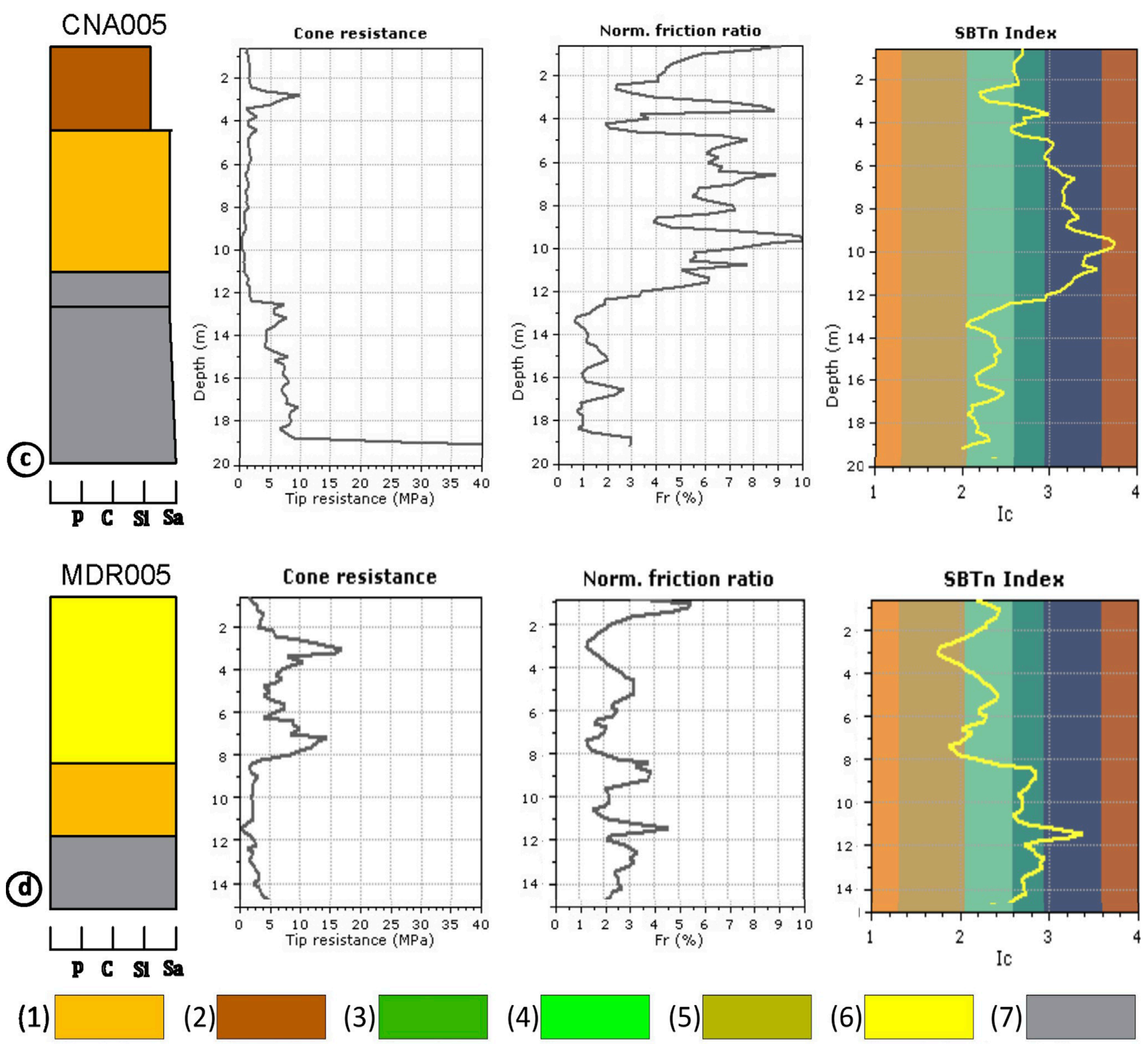

FIGURE 7
(Continued). Reference logs showing the correlation of the various depositional and penetrometric facies of the Volturno delta deposits. i) The ragged logs on the left display the lithologies: p: peat, c: clay, si: silt, and sa: sand, while different colors display the facies association: 1) fluvial channel, 2) floodplain 3) coastal plain, 4) swamp, 5) lagoon, 6) beach-dune, and 7) Late Pleistocene alluvial plain. The plots beside represent the geotechnical characteristics: ii) cone resistance (q_c), iii) normalized friction ratio (*FR*), and iv) normalized soil behavior type index (SBTn).

- The lagoonal facies are composed of two types of lithologies: silt, locally bearing marine fossils, and peaty clays. These variations result in different geotechnical parameters: in the first case, there is a decrease in FR values of the FR, ranging between 0% and 6%, while in peaty clays, the values are higher at 4%–10%; both materials have an average thickness of 1–4 m but have a rather variable depth, which is obviously related to the depositional history of the study area.

Table 2 summarizes the diagnostic features of the facies association, based on the description in Ruberti et al. (2022), along with the pyroclastic sand from the upper part of the tuffaceous substrate. It also includes the q_c and *FR* ranges for each facies association described above.

5 Soil behavior type and facies associations

The abovementioned facies characterized in terms of CPT parameters were plotted on SBTn charts of Robertson (1990). These plots enable a better identification of the specific facies association, most of which fall in distinct I_C ranges (Figure 8). The first graph shows the plot for the fine-grained sediments (i.e., clays and silts, Figure 8a), while the second graph is related to the coarse-grained sediments (Figure 8b). The resulting patterns confirm that homogeneous lithologies may not represent single facies, and these differences are highlighted by geotechnical testing and analysis.

The distributional pattern of each facies in the SBTn plots (Figure 8) reveals specific details on the different geotechnical

10.3389/feart.2025.1585388

TABLE 2 Characterization of the facies and their penetrometic characteristics in the study area.

Depositional system	Facies association	Mean thickness	Lithology and accessories	q_c (MPa)	*FR* %
Late-Pleistocene alluvial plain	Pyroclastic sands	1–7	Gray–brown coarse-to-fine sand pumice and scoriaceous lapilli	5–15	0–3
Alluvial plain	Fluvial channel	2–20	Coarse-to-medium/fine sands	0–10	2–4
	Floodplain	1–10	Clay and silty-clay paleosols, bioturbation	<5	2–10
Delta plain	Coastal plain	1–5	Clay and silts with organic matter, carbonate nodules	<5	3–7
	Swamp	1–3	Soft dark clay peat layers, plant fragments	<5	5–10
	Lagoon	1–4	Silt/sand alternations, shell fragments	<5	0–6
			Peaty clay, bioturbation	<5	4–10
Beach ridge/delta front	Beach-dune	4–12	Yellow medium sands, shell debris	5–15	1–4

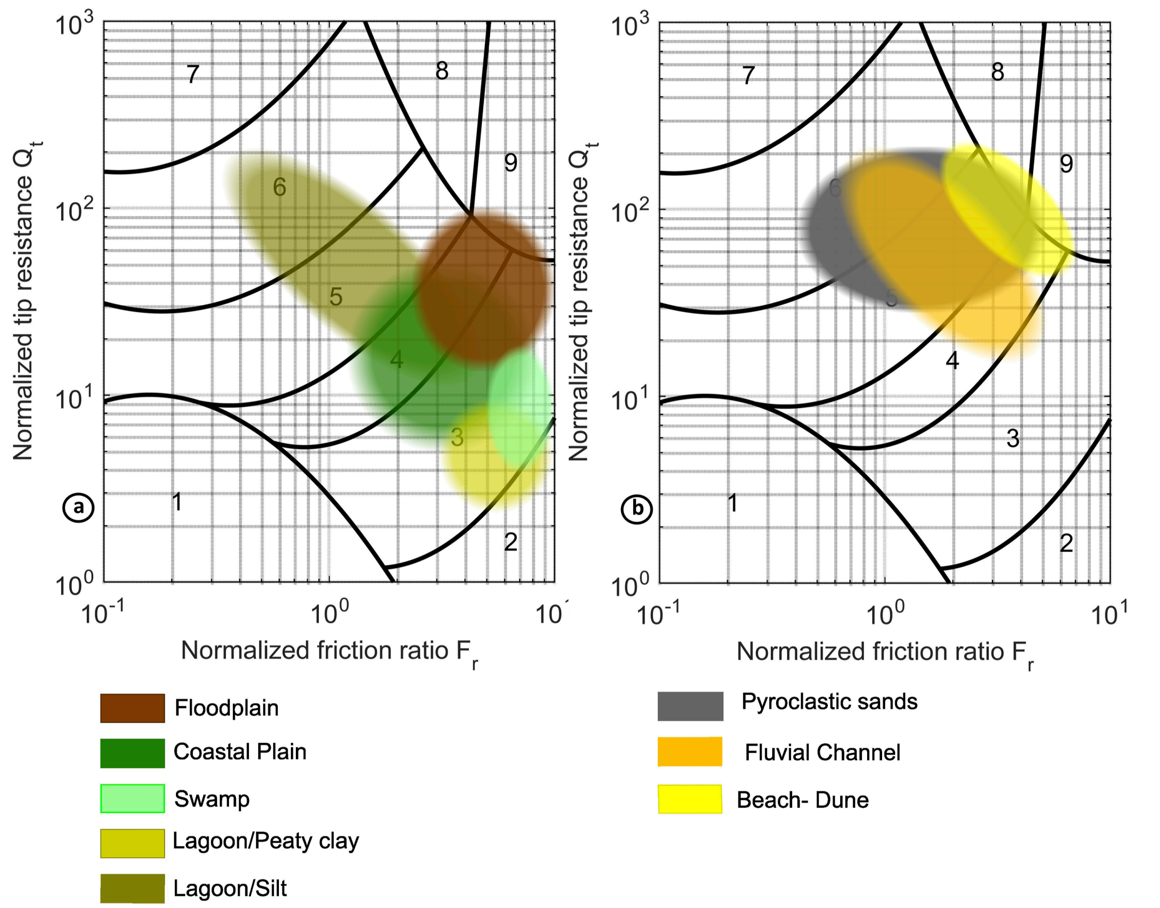

FIGURE 8
Plots of the eight facies on the Robertson (1990) chart. **(a)** Facies association containing fine-grained materials. **(b)** Facies association containing coarse-grained materials. Numbered zones encompass different soil behavior types: 1, sensitive fine-grained soils; 2, organic material; 3, clay; 4, silty clay to clay; 5, clayey silt to silty clay; 6, sandy silt to clayey silt; 7, silty sand to sandy silt; 8, sand to silty sand; 9, sand; 10, gravelly sand to sand; 11, very stiff fine-grained; and 12, sand to clayey sand.

behavior that each specific facies can have. For example, the marked separation of the lagoon lithofacies stands out: the peaty clay belonging to the lagoon exclusively occupies the peat and clay zones (2 and 3) (Figure 8a). In contrast, the silt of the same facies shows a broader range of geotechnical behavior, covering zones 3 through 6; this indicates that various fractions of this loamy material, according to the SBT, exhibit different geotechnical behaviors, ranging from clay (3) to silty mixture (4), sand mixture (5), and sand (6). The floodplain's clayey sediments mainly occupy zones 3 and 4, which are referred to as clay or silt mixtures. In the coastal plain and swamp deposits, there is a partial overlap of geotechnical characteristics. The former presents a broad distribution, partially overlapping with the field of the floodplain, swamp, and lagoon deposits in zones 3 and 4. However, differences between these facies can be found in Q_t values; e.g., the swamp facies are distributed only in zones 2 and 3, i.e., clay and organic clay with lower Q_t values.

The position of the coarse-grained lithofacies on the chart is shown in Figure 8b. The upper surface of the volcanic tuff is often reworked in an alluvial environment, forming gray pyroclastic sands that are, therefore, found only in the deeper portions of the entire Holocene sequence. These sands are distributed across the fields corresponding to silty and sandy mixtures or sand (zones 4, 5, and 6) and to a small extent in zones 8 and 9, where they appear as overconsolidated materials such as stiff sand and stiff fine-grained sand, maintaining relatively constant Q_t values. Partially overlapping with these, the river sands cover zones 4, 5, and 6 and partially zone 3, showing wide variability in both the *FR* and q_c values. A similar trend, but with a narrower distribution, characterizes the beach-dune sands, which cover zones 4 and 5 and partially zones 8 and 9, with a limited range of *FR* values.

6 Discussion and conclusion

The abovementioned approach enables us to distinguish the different depositional facies present in the geological subsurface of the Volturno coastal-deltaic plain and provides insights into their geomechanical properties well beyond the standard lithological geotechnical characterization. Although the use of CPTus to characterize sedimentary facies in modern alluvial and coastal plains has found worldwide application over the last decades (Amorosi and Marchi, 1999; Devincenzi et al., 2004; Lafuerza et al., 2005; Choi and Kim, 2006; Koster et al., 2018; Zhang et al., 2018; Campo et al., 2023), few studies provide a comprehensive characterization of the post-LGM facies associations. Campo et al. (2023) introduced the use of SBT charts to provide a plausible attribution of the sediment type, which also performed well in our case. The different SBT charts of the recognized facies of the Volturno plain provided an acceptable attribution of lithologies to depositional facies association. According to Robertson and Cabal (2022), profiles of I_C provide a simple guide to the continuous variation in soil behavior type in each soil profile based on CPT results. Independent studies have shown that SBT classification typically has greater than 80% reliability when compared with samples, regardless of the soil type. Differences are often due to the presence of soil microstructure (such as aging and bonding).

The results also show that lithofacies of different depositional systems can overlap considerably. Styllas (2014) documented the need to consider additional parameters to characterize facies associations from different depositional systems since their formation is linked to both depositional and post-depositional processes. In our case study, some facies belonging to a specific depositional environment, such as a swamp, show well-defined characteristics distinct from those of other facies. In other cases, corresponding to more complex depositional environments characterized by greater lithological variability, the addition of CPT data interpretation helped in understanding this complexity through the wide range of Q_t and *FR* values that characterize them. This is, for example, the case for the facies of coastal or lagoon environments, in which the lithologies cover a wide range of grain sizes, from clay to sand, and are often thinly intercalated with each other. To overcome this problem, Campo et al. (2023) proposed to use the CPTu curves on a sedimentological basis, examining, for example, the CU (coarsening upward) or FU (fining upward) trends since the sedimentary accumulation processes respond to the sediment supply–accommodation space interaction. Our findings confirm this suggestion, which will support and strengthen the attributions of lithofacies to specific depositional systems and support the still ongoing sequence stratigraphic reconstruction. Furthermore, in the CPTu profiles, it is possible to recognize any thin intercalations of sediments different from the prevailing lithology, which are otherwise lost during standardized drilling operations (mixing and disturbance), thus allowing for the identification of facies transitions that are not clearly evident in the core samples (Törnqvist et al., 2020).

A main finding of our study is, therefore, the demonstration that while different facies associations may share similar lithologic compositions, their geotechnical behaviors may be strikingly dissimilar. This important fact is also reflected in the large variability in the subsidence rates, in combination with the sediment age, its depositional history, and degree of consolidation, which strongly determines its contemporary geotechnical properties. In general, younger sediments exhibit less contemporary consolidation, making them more compressible and prone to (auto)compaction. In contrast, older sediments have experienced more and longer consolidation processes, resulting in higher shear strength and greater stability (Murakami, 1988). The overburden can influence the degree of compaction at depth (Törnqvist et al., 2008); the same holds true for the depositional history, either in terms of age or sedimentation rates through the whole column, whether in recent or older deposits (Zoccarato et al., 2018). Another important aspect is related to peat-rich deposits. The long-term self-compaction of peat deposits is controlled by the composition and structure, which, in turn, control both the *in situ* void ratio at which a soil reaches equilibrium and the compressibility after the soil structure yields at the preconsolidation pressure. The composition of the soil, mainly the mineralogy of the particles, is the most important factor that directly determines both wo (initial water content) and Cc (compression index). Peat deposits reach equilibrium at high water contents of 200%–1,500% and display values of Cc typically in the range of 2–12 because a large amount of water is held within and among the particles (*cf.* Terzaghi et al., 1996). It follows that large primary consolidation settlements are expected for any changes in effective vertical stress.

It should be noted that the overall results may be affected by the spatial representativeness of the testing networks: the alluvial and coastal–deltaic depositional contexts are characterized by the wide variability of facies over short distances and in time. Furthermore, dating is fundamental for facies correlation. However, the Holocene succession outcropping in our study area accumulated immediately on a relatively stable Pleistocene basement characterized by tuff, and therefore, all measurements are strictly related to the Holocene sequence.

On the whole, our new CPT data and geomechanical quantification of the Holocene sedimentary sequence of the Volturno delta plain enable further future explorations, for example, to simulate 3D Holocene delta growth and evolutionary sediment compaction using the NATSUB3D model (Xotta et al., 2022). This simulator enables the simulation of aggradation, progradation, and self-compaction of depositional systems (Zoccarato and Teatini, 2017; Zoccarato et al., 2018), thus modeling the long-term evolution of sedimentary landforms, as showcased recently for the Holocene Mekong delta (Baldan et al., 2024). Apart from unlocking these exciting and valuable research opportunities for the Volturno delta plain, our results underscore that CPTs provide an excellent resource to support stratigraphic analysis, while our transferable approach offers new insights into the compressibility of individual facies that characterize a coastal-deltaic and alluvial setting.

Finally, with respect to coastal-deltaic subsidence, this approach highlights the importance of management of all this information in a geo-database, which then becomes a useful tool for the elaboration of potential subsidence maps on even large areas, where the great variability of lithofacies present determines differential subsidence.

Data availability statement

The raw data supporting the conclusions of this article will be made available by the authors, without undue reservation.

Author contributions

CB: Data curation, Formal analysis, Investigation, Methodology, Software, and Writing – original draft. PM: Conceptualization, Methodology, Supervision, Validation, Writing – original draft, and Writing – review and editing. AM: Formal analysis, Methodology, Supervision, and Writing – original draft. DR: Conceptualization, Data curation, Methodology, Resources, Supervision, Validation, Visualization, Writing – original draft, and Writing – review and editing.

Funding

The author(s) declare that no financial support was received for the research and/or publication of this article.

Conflict of interest

The authors declare that the research was conducted in the absence of any commercial or financial relationships that could be construed as a potential conflict of interest.

Generative AI statement

The author(s) declare that no Generative AI was used in the creation of this manuscript.

Publisher's note

All claims expressed in this article are solely those of the authors and do not necessarily represent those of their affiliated organizations, or those of the publisher, the editors and the reviewers. Any product that may be evaluated in this article, or claim that may be made by its manufacturer, is not guaranteed or endorsed by the publisher.

References

Amato, V., Aucelli, P. P. C., Corrado, G., Paola, G.D., Matano, F., Pappone, G., et al. (2020). Comparing geological and Persistent Scatterer Interferometry data of the Sele River coastal plain, southern Italy: implications for recent subsidence trends. *Geomorphology* 351, 106953. doi:10.1016/j.geomorph.2019.106953

Amorosi, A., and Marchi, N. (1999). High-resolution sequence stratigraphy from piezocone tests: an example from the Late Quaternary deposits of the southeastern Po Plain. *Sediment. Geol.* 128, 67–81. doi:10.1016/S0037-0738(99)00062-7

Amorosi, A., Molisso, F., Pacifico, A., Rossi, V., Ruberti, D., Sacchi, M., et al. (2013). The Holocene evolution of the Volturno River coastal plain (southern Italy). *J. Mediterr. Earth Sci.* 5, 7–11.

Amorosi, A., Pacifico, A., Rossi, V., and Ruberti, D. (2012). Late Quaternary incision and deposition in an active volcanic setting: the Volturno valley fill, southern Italy. *Sediment. Geol.* 282, 307–320. doi:10.1016/j.sedgeo.2012.10.003

Anagnostopoulos, A., Koukis, G., Sabatakakis, N., and Tsiambaos, G. (2003). Empirical correlations of soil parameters based on Cone Penetration Tests (CPT) for Greek soils. *Geotechnical Geol. Eng.* 21, 377–387. doi:10.1023/B:GEGE.0000006064.47819.1a

Anthony, E., Syvitski, J., Zăinescu, F., Nicholls, R. J., Cohen, K. M., Marriner, N., et al. (2024). Delta sustainability from the Holocene to the Anthropocene and envisioning the future. *Nat. Sustain.* 7, 1235–1246. doi:10.1038/s41893-024-01426-3

Aucelli, P. P. C., Paola, G.D., Incontri, P., Rizzo, A., Vilardo, G., Benassai, G., et al. (2017). Coastal inundation risk assessment due to subsidence and sea level rise in a Mediterranean alluvial plain (Volturno coastal plain – southern Italy). *Estuar. Coast. Shelf Sci.* 198, 597–609. doi:10.1016/j.ecss.2016.06.017

Bagheri-Gavkosh, M., Hosseini, S. M., Ataie-Ashtiani, B., Sohani, Y., Ebrahimian, H., Morovat, F., et al. (2021). Land subsidence: a global challenge. *Sci. Total Environ.* 778, 146193. doi:10.1016/j.scitotenv.2021.146193

Baldan, S., Minderhoud, P. S. J., Xotta, R., Zoccarato, C., and Teatini, P. (2024). Data-driven 3D modelling of long-term Holocene delta evolution and sediment compaction: the mekong delta. *Earth Surf. Process. Landforms* 50. doi:10.1002/esp.6046

Becker, M., Seeger, K., Paszkowski, A., Marcos, M., Papa, F., Almar, R., et al. (2024). Coastal flooding in Asian megadeltas: recent advances, persistent challenges, and call for actions amidst local and global changes. *Rev. Geophys.* 62, e2024RG000846. doi:10.1029/2024RG000846

Begemann, H. K. S. P. (1965). The friction jacket cone as an aid in determining the soil profile. In: Proceedings of the 6th international conference on soil mechanics and foundation engineering; 1965 September 8–15; Montreal, Canada. Toronto, Canada: University of Toronto Press, 17–20.

Bombasaro, E., and Kasper, T. (2016). Evaluation of spatial soil variability in the Pearl River Estuary using CPTU data. *Soils Found.* 56, 496–505. doi:10.1016/j.sandf.2016.04.015

Boumpoulis, V., Depountis, N., Pelekis, P., and Sabatakakis, N. (2021). SPT and CPT application for liquefaction evaluation in Greece. *Arabian J. Geosciences* 14, 1631. doi:10.1007/s12517-021-08103-1

Bozzano, F., Esposito, C., Franchi, S., Mazzanti, P., Perissin, D., Rocca, A., et al. (2015). Analysis of a subsidence process by integrating geological and hydrogeological modelling with satellite InSAR data. In: Editors. *Engineering geology for society and territory*. G. Lollino, A. Manconi, F. Guzzetti, M. Culshaw, P. Bobrowsky, F. Luino, et al. Cham, Switzerland: Springer International Publishing, 5, 155–159. doi:10.1007/978-3-319-09048-1_31

Brückner, H., Vött, A., Schriever, A., and Handl, M. (2005). Holocene delta progradation in the eastern Mediterranean – case studies in their historical context. *Méditerranée N°1* 2, 95–106. doi:10.4000/mediterranee.2342

Bruno, L., Campo, B., Costagli, B., Stouthamer, E., Teatini, P., Zoccarato, C., et al. (2020). Factors controlling natural subsidence in the Po Plain. *Proc. Int. Assoc. Hydrological Sci.* 382, 285–290. doi:10.5194/piahs-382-285-2020

Buffardi, C., Barbato, R., Vigliotti, M., Mandolini, A., and Ruberti, D. (2021). The holocene evolution of the volturno coastal plain (Northern campania, southern Italy): implications for the understanding of subsidence patterns. *Water* 13, 2692. doi:10.3390/w13192692

Buffardi, C., and Ruberti, D. (2023). The issue of land subsidence in coastal and alluvial plains: a bibliometric review. *Remote Sens.* 15, 2409. doi:10.3390/rs15092409

Buisman, A. S. (1940). Grondmechanica. In: *Toegepaste mechanica*. Milton Park, Oxfordshire: Taylor and Francis.

Busico, G., Buffardi, C., Ntona, M. M., Vigliotti, M., Colombani, N., Mastrocicco, M., et al. (2021). Actual and forecasted vulnerability assessment to seawater intrusion via galdit-susi in the volturno river mouth (Italy). *Remote Sens.* 13, 3632. doi:10.3390/rs13183632

Cai, Y., Li, J., Li, X., Li, D., and Zhang, L. (2019). Estimating soil resistance at unsampled locations based on limited CPT data. *Bull. Eng. Geol. Environ.* 78, 3637–3648. doi:10.1007/s10064-018-1318-2

Calabrese, L., Luciani, P., and Perini, L. (2021). A review of impact of subsidence induced by gas exploitation on costal erosion in Emilia-Romagna, Italy. *Bull. Geophys. Oceanogr.* 62, 279–300. doi:10.4430/bgta0356

Campo, B., Bruno, L., and Amorosi, A. (2023). Sedimentary facies characterization through CPTU profiles: an effective tool for subsurface investigation of modern alluvial and coastal plains. *Sedimentology* 70, 1302–1327. doi:10.1111/sed.13079

Campolunghi, M. P., Capelli, G., Funiciello, R., and Lanzini, M. (2007). Geotechnical studies for foundation settlement in Holocenic alluvial deposits in the City of Rome (Italy). *Eng. Geol.* 89, 9–35. doi:10.1016/j.enggeo.2006.08.003

Carbognin, L., Teatini, P., Tomasin, A., and Tosi, L. (2010). Global change and relative sea level rise at Venice: what impact in term of flooding. *Clim. Dyn.* 35, 1039–1047. doi:10.1007/s00382-009-0617-5

Choi, K., and Kim, J. H. (2006). Identifying late Quaternary coastal deposits in Kyonggi Bay, Korea, by their geotechnical properties. *Geo-Marine Lett.* 26, 77–89. doi:10.1007/s00367-006-0018-2

Coelho, C., Silva, R., Veloso-Gomes, F., and Taveira-Pinto, F. (2009). Potential effects of climate change on northwest Portuguese coastal zones. *ICES J. Mar. Sci.* 66, 1497–1507. doi:10.1093/icesjms/fsp132

Colombani, N., Alessandrino, L., Gaiolini, M., Gervasio, M. P., Ruberti, D., and Mastrocicco, M. (2024). Unravelling the salinity origins in the coastal aquifer/aquitard system of the Volturno River (Italy). *Water Res.* 263, 122145. doi:10.1016/j.watres.2024.122145

Corrado, G., Amodio, S., Aucelli, P. P. C., Pappone, G., and Schiattarella, M. (2020). The subsurface geology and landscape evolution of the volturno Coastal Plain, Italy: interplay between tectonics and sea-level changes during the quaternary. *Water* 12, 3386. doi:10.3390/w12123386

Da Lio, C., and Tosi, L. (2018). Land subsidence in the Friuli Venezia Giulia coastal plain, Italy: 1992–2010 results from SAR-based interferometry. *Sci. Total Environ.* 633, 752–764. doi:10.1016/j.scitotenv.2018.03.244

Dassargues, A., Biver, P., and Monjoie, A. (1991). Geotechnical properties of the quaternary sediments in shanghai. *Eng. Geol.* 31, 71–90. doi:10.1016/0013-7952(91)90058-S

Devillers, B., Bony, G., Degeai, J.-P., Gascò, J., Lachenal, T., Bruneton, H., et al. (2019). Holocene coastal environmental changes and human occupation of the lower Hérault River, southern France. *Quat. Sci. Rev.* 222, 105912. doi:10.1016/j.quascirev.2019.105912

Devincenzi, M. J., Colas, S., Casamor, J. L., Canals, M., Falivene, O., and Busquets, P. (2004). High resolution stratigraphic and sedimentological analysis of Llobregat delta nearby Barcelona from CPT and CPTU tests. Proc. 2 nd International Conference on Site Characterization ISC'2, Porto. Vol 1. Millpress, Rotterdam. *Geotechnical Geophys. Site Characterisation ISC-2* 1, 877–884.

Donadio, C., Vigliotti, M., Valente, R., Stanislao, C., Ivaldi, R., and Ruberti, D. (2018). Anthropic vs. natural shoreline changes along the northern Campania coast, Italy. *J. Coast. Conservation* 22, 939–955. doi:10.1007/s11852-017-0563-z

El-Reedy, M. A. (2015). Geotechnical data and piles design. In: *Marine structural design calculations*. Amsterdam, Netherlands: Elsevier, 217–280. doi:10.1016/B978-0-08-099987-6.00006-4

Ericson, J. P., Vörösmarty, C. J., Dingman, S. L., Ward, L. G., and Meybeck, M. (2006). Effective sea-level rise and deltas: causes of change and human dimension implications. *Glob. Planet. Change* 50, 63–82. doi:10.1016/j.gloplacha.2005.07.004

Eslami, A., Moshfeghi, S., MolaAbasi, H., and Eslami, M. M. (2020). CPT equipment, performance, and records. In: *Piezocone and cone penetration test (CPTu and CPT) applications in foundation engineering*. Amsterdam, Netherlands: Elsevier, 55–80. doi:10.1016/B978-0-08-102766-0.00003-1

Galloway, D. L., Jones, D. R., and Ingebritsen, S. E. (2000). *Measuring land subsidence from space*. Reston, Virginia: US Department of the Interior, US Geological Survey. GS fact sheet-051-00 1–4.

Galloway, D. L., and Burbey, T. J. (2011). Review: regional land subsidence accompanying groundwater extraction. *Hydrogeology J.* 19, 1459–1486. doi:10.1007/s10040-011-0775-5

Geyin, M., Maurer, B. W., Bradley, B. A., Green, R. A., and Ballegooy, S. van (2021). CPT-based liquefaction case histories compiled from three earthquakes in Canterbury, New Zealand. *Earthq. Spectra* 37, 2920–2945. doi:10.1177/8755293021996367

Guan, Z., Wang, Y., and Zhao, T. (2021). Delineating the spatial distribution of soil liquefaction potential in a cross-section from limited cone penetration tests. *Soil Dyn. Earthq. Eng.* 145, 106710. doi:10.1016/j.soildyn.2021.106710

Guo, L., Liu, X., Yang, Z., Jia, C., Shi, W., and Ling, X. (2022). CPT-based analysis of structured soil characteristics and liquefaction failure of the Yellow River Subaquatic Delta. *Mar. Georesources and Geotechnol.* 40, 308–320. doi:10.1080/1064119X.2021.1891589

Heidarie Golafzani, S., Eslami, A., and Jamshidi Chenari, R. (2020). Probabilistic assessment of model uncertainty for prediction of pile foundation bearing capacity; static analysis, SPT and CPT-based methods. *Geotechnical Geol. Eng.* 38, 5023–5041. doi:10.1007/s10706-020-01346-x

Herrera-García, G., Ezquerro, P., Tomas, R., Béjar-Pizarro, M., López-Vinielles, J., Rossi, M., et al. (2021). Mapping the global threat of land subsidence. *Science* 371, 34–36. doi:10.1126/science.abb8549

Higgins, S. A. (2016). Review: advances in delta-subsidence research using satellite methods. *Hydrogeology J.* 24, 587–600. doi:10.1007/s10040-015-1330-6

Higgins, S. A., Overeem, I., Steckler, M. S., Syvitski, J. P. M., Seeber, L., and Akhter, S. H. (2014). InSAR measurements of compaction and subsidence in the Ganges-Brahmaputra Delta, Bangladesh. *J. Geophys. Res. Earth Surf.* 119, 1768–1781. doi:10.1002/2014JF003117

Hu, R. L., Yue, Z. Q., Wang, L. C., and Wang, S. J. (2004). Review on current status and challenging issues of land subsidence in China. *Eng. Geol.* 76, 65–77. doi:10.1016/j.enggeo.2004.06.006

Huning, L. S., Love, C. A., Anjileli, H., Vahedifard, F., Zhao, Y., Chaffe, P. L. B., et al. (2024). Global land subsidence: impact of climate extremes and human activities. *Rev. Geophys.* 62. doi:10.1029/2023RG000817

Idriss, I. M., and Boulanger, R. W. (2006). Semi-empirical procedures for evaluating liquefaction potential during earthquakes. *Soil Dyn. Earthq. Eng.* 26, 115–130. doi:10.1016/j.soildyn.2004.11.023

Jones, C. E., An, K., Blom, R. G., Kent, J. D., Ivins, E. R., and Bekaert, D. (2016). Anthropogenic and geologic influences on subsidence in the vicinity of New Orleans, Louisiana. *J. Geophys. Res. Solid Earth* 121, 3867–3887. doi:10.1002/2015JB012636

Koster, K., Erkens, G., and Zwanenburg, C. (2016). A new soil mechanics approach to quantify and predict land subsidence by peat compression. *Geophys. Res. Lett.* 43 (10), 792–10. doi:10.1002/2016GL071116

Koster, K., Lange, G. De, Harting, R., Heer, E. de, and Middelkoop, H. (2018). Characterizing void ratio and compressibility of Holocene peat with CPT for assessing coastal-deltaic subsidence. *Q. J. Eng. Geol. Hydrogeology* 51, 210–218. doi:10.1144/qjegh2017-120

Lafuerza, S., Canals, M., Casamor, J. L., and Devincenzi, J. M. (2005). Characterization of deltaic sediment bodies based on *in situ* CPT/CPTU profiles: a case study on the Llobregat delta plain, Barcelona, Spain. *Mar. Geol.* 497–510. doi:10.1016/j.margeo.2005.06.043

Lazarus, E. D., Ellis, M. A., Brad Murray, A., and Hall, D. M. (2016). An evolving research agenda for human–coastal systems. *Geomorphology* 256, 81–90. doi:10.1016/j.geomorph.2015.07.043

Liu, Y., and Huang, H.-J. (2013). Characterization and mechanism of regional land subsidence in the Yellow River Delta, China. *Nat. Hazards* 68, 687–709. doi:10.1007/s11069-013-0648-4

Margaritelli, G., Vallefuoco, M., Rita, F. Di, Capotondi, L., Bellucci, L. G., Insinga, D. D., et al. (2016). Marine response to climate changes during the last five millennia in the central Mediterranean Sea. *Glob. Planet. Change* 142, 53–72. doi:10.1016/j.gloplacha.2016.04.007

Matano, F., Sacchi, M., Vigliotti, M., and Ruberti, D. (2018). Subsidence trends of Volturno river coastal plain (Northern Campania, Southern Italy) inferred by sar interferometry data. *Geosci.* 8, 8. doi:10.3390/geosciences8010008

Meckel, T. A., Brink, U.S. ten, and Williams, S. J. (2006). Current subsidence rates due to compaction of Holocene sediments in southern Louisiana. *Geophys. Res. Lett.* 33, 1–5. doi:10.1029/2006GL026300

Mentaschi, L., Vousdoukas, M. I., Pekel, J.-F., Voukouvalas, E., and Feyen, L. (2018). Global long-term observations of coastal erosion and accretion. *Sci. Rep.* 8, 12876. doi:10.1038/s41598-018-30904-w

Miall, A. D. (2018). Depositional environments. In: R. Sorkhabi, editor. *Encyclopedia of petroleum geoscience. Encyclopedia of earth sciences series*. Cham, Switzerland: Springer, 1–16. doi:10.1007/978-3-319-02330-4_138-1

Minderhoud, P. S. J., Coumou, L., Erban, L. E., Middelkoop, H., Stouthamer, E., and Addink, E. A. (2018). The relation between land use and subsidence in the Vietnamese Mekong delta. *Sci. Total Environ.* 634, 715–726. doi:10.1016/j.scitotenv.2018.03.372

Misuraca, M., Budillon, F., Tonielli, R., Martino, G. Di, Innangi, S., and Ferraro, L. (2018). Coastal evolution, hydrothermal migration pathways and soft deformation along the campania continental shelf (Southern tyrrhenian sea): insights from high-resolution seismic profiles. *Geosci. Switz.* 8, 121. doi:10.3390/geosciences8040121

Mohammad, L. N., Titi, H. H., and Herath, A. (1999). Evaluation of resilient modulus of subgrade soil by cone penetration test. *Transp. Res. Rec. J. Transp. Res. Board* 1652, 236–245. doi:10.3141/1652-30

Murakami, Y. (1988). Secondary compression in the stage of primary consolidation. *Soils and Foundations* 28, 169–174. doi:10.3208/sandf1972.28.3_169

Pedretti, L., Giarola, A., Korff, M., Lambert, J., and Meisina, C. (2024). Comprehensive database of land subsidence in 143 major coastal cities around the world: overview of issues, causes, and future challenges. *Front. Earth Sci.* 12. doi:10.3389/feart.2024.1351581

Phien-wej, N., Giao, P. H., and Nutalaya, P. (2006). Land subsidence in bangkok, Thailand. *Thailand* 82, 187–201. doi:10.1016/j.enggeo.2005.10.004

Ranasinghe, R. (2020). On the need for a new generation of coastal change models for the 21st century. *Sci. Rep.* 10, 2010. doi:10.1038/s41598-020-58376-x

Robertson, P. K. (1990). Soil classification using the cone penetration test. *Can. Geotechnical J.* 27, 151–158. doi:10.1139/t90-014

Robertson, P. K. (2010). Soil behaviour type from the CPT: an update. In: *2nd international symposium on cone penetration testing, huntington beach*, 2. Signal Hill, California: Gregg Drilling and Testing Inc.

Robertson, P. K. (2016). Cone penetration test (CPT)-based soil behaviour type (SBT) classification system — an update. *Can. Geotechnical J.* 53, 1910–1927. doi:10.1139/cgj-2016-0044

Robertson, P. K., and Cabal, K. (2022). *Guide to cone penetration testing*. 7th edition. Edmonton, Canada: P.K. Robertson Consulting, 163.

Romano, P., Santo, A., and Voltaggio, M. (1994). L'evoluzione geomorfologica della pianura del fiume Volturno (Campania) durante il tardo Quaternario (Pleistocene Medio-Superiore - Olocene). *Alp. Mediterr. Quat.* 7, 41–55.

Roviello, V., Cesare, M. De, D'Onofrio, A., Gialanella, L., Guan, Y. J., Roos, P., et al. (2020). New analytical methods for the assessment of natural (238U, 232Th, 226Ra, 40K) and anthropogenic (137Cs) radionuclides as actinides (239Pu, 240Pu): the case study of the Garigliano NPP releases along the Domitia sandy beaches (Southern Italy). *CATENA* 193, 104612. doi:10.1016/j.catena.2020.104612

Ruberti, D., Buffardi, C., Sacchi, M., and Vigliotti, M. (2022). The late Pleistocene-Holocene changing morphology of the Volturno delta and coast (northern Campania, Italy): geological architecture and human influence. *Quat. Int.* 625, 14–28. doi:10.1016/j.quaint.2022.03.023

Ruberti, D., Mandolini, A., Matano, F., Picarelli, L., and Sacchi, M. (2017). Holocene stratigraphic architecture and current land subsidence of the Volturno coastal plain (northern Campania, southern Italy). *J. Mediterr. Earth Sci.* 9, 193–196.

Ruberti, D., Sacchi, M., Pepe, f., and Vigliotti, M. (2018b). LGM incised valley in a volcanic setting. The northern Campania Plain (Southern Italy). *Alp. Mediterr. Quat.* 31, 35–38. Available online at: https://amq.aiqua.it/index.php/amq/article/view/183.

Ruberti, D., and Vigliotti, M. (2017). Land use and landscape pattern changes driven by land reclamation in a coastal area: the case of Volturno delta plain, Campania Region, southern Italy. *Environ. Earth Sci.* 76, 694. doi:10.1007/s12665-017-7022-x

Ruberti, D., Vigliotti, M., Marzaioli, R., Pacifico, A., and Ermice, A. (2014). Stratigraphic architecture and anthropic impacts on subsoil to assess the intrinsic potential vulnerability of groundwater: the northeastern Campania Plain case study, southern Italy. *Environ. Earth Sci.* 71, 319–339. doi:10.1007/s12665-013-2436-6

Ruberti, D., Vigliotti, M., Mauro, A. Di, Chieffi, R., and Natale, M.Di (2018a). Human influence over 150 years of coastal evolution in the Volturno delta system (southern Italy). *J. Coast. Conservation* 22, 897–917. doi:10.1007/s11852-017-0557-x

Ruberti, D., Vigliotti, M., Rolandi, R., and Lascio, M. Di (2020). 9-Effect of paleomorphology on facies distribution of the Campania Ignimbrite in the northern Campania Plain, southern Italy. In: *Vesuvius, Campi Flegrei, and campanian volcanism*. Editors B. De. Vivo, H. Belkin, and G. Rolandi, Amsterdam, Netherlands: Elsevier, 207–229. doi:10.1016/B978-0-12-816454-9.00009-2

Sacchi, M., Molisso, F., Pacifico, A., Vigliotti, M., Sabbarese, C., and Ruberti, D. (2014). Late-Holocene to recent evolution of Lake Patria, South Italy: an example of a coastal lagoon within a Mediterranean delta system. *Glob. Planet. Change* 117, 9–27. doi:10.1016/j.gloplacha.2014.03.004

Santangelo, N., Ciampo, G., Donato, V. Di, Esposito, P., Petrosino, P., Romano, P., et al. (2010). Late quaternary buried lagoons in the northern campania plain (southern Italy): evolution of a coastal system under the influence of volcano-tectonics and eustatism. *Italian J. Geosciences* 129, 156–175. doi:10.3301/IJG.2009.12

Santangelo, N., Romano, P., Ascione, A., and Russo Ermolli, E. (2017). Quaternary evolution of the Southern Apennines coastal plains: a review. *Geol. Carpathica* 68, 43–56. doi:10.1515/geoca-2017-0004

Sarti, G., Rossi, V., and Amorosi, A. (2012). Influence of Holocene stratigraphic architecture on ground surface settlements: a case study from the City of Pisa (Tuscany, Italy). *Sediment. Geol.* 281, 75–87. doi:10.1016/j.sedgeo.2012.08.008

Schmitt, R. J. P., and Minderhoud, P. S. J. (2023). Data, knowledge, and modeling challenges for science-informed management of river deltas. *One Earth* 6 (3), 216–235. doi:10.1016/j.oneear.2023.02.010

Scown, M. W., Dunn, F. E., Dekker, S. C., van Vuuren, D. P., Karabil, S., Sutanudjaja, E. H., et al. (2023). Global change scenarios in coastal river deltas and their sustainable development implications. *Glob. Environ. Change* 82, 102736. doi:10.1016/j.gloenvcha.2023.102736

Shirzaei, M., Freymueller, J., Törnqvist, T. E., Galloway, D. L., Dura, T., and Minderhoud, P. S. J. (2021). Measuring, modelling and projecting coastal land subsidence. *Nat. Rev. Earth Environ.* 2, 40–58. doi:10.1038/s43017-020-00115-x

Stiros, S. C. (2001). Subsidence of the Thessaloniki (northern Greece) coastal plain, 1960–1999. *Eng. Geol.* 61, 243–256. doi:10.1016/S0013-7952(01)00027-8

Stouthamer, E., Erkens, G., Cohen, K., Hegger, D., Driessen, P., PeterWeikard, H., et al. (2020). Dutch national scientific research program on land subsidence: living on soft soils subsidence and society. *Proc. Int. Assoc. Hydrological Sci.* 382, 815–819. doi:10.5194/PIAHS-382-815-2020

Styllas, M. (2014). A simple approach to define Holocene sequence stratigraphy using borehole and cone penetration test data. *Sedimentology* 61, 444–460. doi:10.1111/sed.12061

Switzer, A. D., Sloss, C. R., Horton, B. P., and Zong, Y. (2012). Preparing for coastal change. *Quat. Sci. Rev.* 54, 1–3. doi:10.1016/j.quascirev.2012.09.005

Syvitski, J., Anthony, E., Saito, Y., Zăinescu, F., Day, J., Bhattacharya, J. P., et al. (2022). Large deltas, small deltas: toward a more rigorous understanding of coastal marine deltas. *Glob. Planet. Change* 218, 103958. doi:10.1016/j.gloplacha.2022.103958

Syvitski, J., Kettner, A., Overeem, I., Hutton, E. W. H., Hannon, M. T., Brakenridge, G. R., et al. (2009). Sinking deltas due to human activities. *Nat. Geosci.* 2, 681–686. doi:10.1038/ngeo629

Teatini, P., Tosi, L., and Strozzi, T. (2011). Quantitative evidence that compaction of Holocene sediments drives the present land subsidence of the Po Delta, Italy. *J. Geophys. Res.* 116, B08407. doi:10.1029/2010JB008122

Teatini, P., Tosi, L., Strozzi, T., Carbognin, L., Cecconi, G., Rosselli, R., et al. (2012). Resolving land subsidence within the Venice Lagoon by persistent scatterer SAR interferometry. *Phys. Chem. Earth.* 40-41, 72–79. doi:10.1016/j.pce.2010.01.002

Terzaghi, K., Peck, R. B., and Mesri, G. (1996). *Soil mechanics in engineering practice*. 3rd Edition. New York, NY: John Wiley and Sons, Inc.

Thomas, F., Livio, F. A., Ferrario, F., Pizza, M., and Chalaturnyk, R. (2024). A review of subsidence monitoring techniques in offshore environments. *Sensors* 24, 4164. doi:10.3390/s24134164

Törnqvist, T. E., Jankowski, K. L., Li, Y.-X., and González, J. L. (2020). Tipping points of Mississippi Delta marshes due to accelerated sea-level rise. *Sci. Adv.* 6, eaaz5512. doi:10.1126/sciadv.aaz5512

Törnqvist, T. E., Wallace, D. J., Storms, J. E. A., Wallinga, J., Dam, R. L. V., Blaauw, M., et al. (2008). Mississippi Delta subsidence primarily caused by compaction of Holocene strata. *Nat. Geosci.* 1, 173–176. doi:10.1038/ngeo129

Tosi, L., Lio, C. Da, Teatini, P., and Strozzi, T. (2018). Land subsidence in coastal environments: knowledge advance in the Venice coastland by TerraSAR-X PSI. *Remote Sens.* 10, 1191. doi:10.3390/rs10081191

Tzampoglou, P., and Loupasakis, C. (2018). Evaluating geological and geotechnical data for the study of land subsidence phenomena at the perimeter of the Amyntaio coalmine, Greece. *Int. J. Min. Sci. Technol.* 28, 601–612. doi:10.1016/j.ijmst.2017.11.002

van Asselen, S. (2011). The contribution of peat compaction to total basin subsidence: implications for the provision of accommodation space in organic-rich deltas. *Basin Res.* 23, 239–255. doi:10.1111/j.1365-2117.2010.00482.x

van Asselen, S., Karssenberg, D., and Stouthamer, E. (2011). Contribution of peat compaction to relative sea-level rise within Holocene deltas. *Geophys. Res. Lett.* 38, L24401–5pp. doi:10.1029/2011GL049835 van Asselen, S., Stouthamer, E., and van Asch, T. W. J. (2009). Effects of peat compaction on delta evolution: a review on processes, responses, measuring and modeling. *Earth-Science Rev.* 92, 35–51. doi:10.1016/j.earscirev.2008.11.001

Vardon, P. J., and Peuchen, J. (2021). CPT correlations for thermal properties of soils. *Acta Geotech.* 16, 635–646. doi:10.1007/s11440-020-01027-2

Verde, R., Vigliotti, M., Prevedello, L., Sprovieri, M., and Ruberti, D. (2013). An integrated approach to environmental quality assessment in a coastal setting in Campania (Southern Italy). *Environ. Earth Sci.* 70, 407–424. doi:10.1007/s12665-012-2136-7

Vivo, B. De, Rolandi, G., Gans, P. B., Calvert, A., Bohrson, W. A., Spera, F. J., et al. (2001). New constraints on the pyroclastic eruptive history of the Campanian volcanic Plain (Italy). *Mineralogy Petrology* 73, 47–65. doi:10.1007/s007100170010

Wu, P. C., Wei, M., and D'Hondt, S. (2022). Subsidence in coastal cities throughout the world observed by InSAR. *Geophys. Res. Lett.* 49. doi:10.1029/2022GL098477

Xotta, R., Zoccarato, C., Minderhoud, P. S. J., and Teatini, P. (2022). Modeling the role of compaction in the three-dimensional evolution of depositional environments. *J. Geophys. Res. Earth Surf.* 127. doi:10.1029/2022JF006590

Yang, J. L., Cao, G., Li, H., Li, J., Hu, Y. Z., Xu, Q. M., et al. (2014). Study of natural consolidation of Late Cenozoic era clay and land subsidence in Tianjin coastal area. *Yantu Lixue/Rock Soil Mech.* 35, 2579–2586.

Yang, Z., Liu, X., Guo, L., Cui, Y., Su, X., and Ling, X. (2021). Soil classification and site variability analysis based on cpt—a case study in the yellow river subaquatic delta, China. *J. Mar. Sci. Eng.* 9, 431. doi:10.3390/jmse9040431

Zhang, X., Lin, C.-M., Dalrymple, R. W., Gao, S., and Canas, D. T. (2018). Use of the Cone Penetration Testing (CPT) method to interpret late Quaternary tide-dominated successions: a case study from the eastern China coastal plain. *Cont. Shelf Res.* 161, 49–57. doi:10.1016/j.csr.2018.03.012

Zhao, Z., Duan, W., Cai, G., Wu, M., and Liu, S. (2022). CPT-based fully probabilistic seismic liquefaction potential assessment to reduce uncertainty: integrating XGBoost algorithm with Bayesian theorem. *Comput. Geotechnics* 149, 104868. doi:10.1016/j.compgeo.2022.104868

Zoccarato, C., Minderhoud, P. S. J., and Teatini, P. (2018). The role of sedimentation and natural compaction in a prograding delta: insights from the mega Mekong delta, Vietnam. *Sci. Rep.* 8, 11437. doi:10.1038/s41598-018-29734-7

Zoccarato, C., and Teatini, P. (2017). Numerical simulations of Holocene salt-marsh dynamics under the hypothesis of large soil deformations. *Adv. Water Resour.* 110, 107–119. doi:10.1016/j.advwatres.2017.10.006